Impact of the updating scheme on stationary states of networks

Impact of the updating scheme on stationary states of networks

F Radicchi[1], Y Y Ahn[2] and H Meyer-Ortmanns[3]

[1] Complex Networks Lagrange Laboratory (CNNL), ISI Foundation, Viale S Severo 65, 10133 Torino, Italy
[2] Department of Physics, Korea Advanced Institute of Science and Technology, Daejeon 305-701, Korea
[3] School of Engineering and Science, Jacobs University, PO Box 750561, D-28725 Bremen, Germany

E-mail: h.ortmanns@jacobs-university.de

Abstract
From Boolean networks it is well known that the number of attractors as a function of the system size depends on the updating scheme which is chosen either synchronously or asynchronously. In this contribution, we report on a systematic interpolation between synchronous and asynchronous updating in a one-dimensional chain of Ising spins. The stationary state for fully synchronous updating is antiferromagnetic. The interpolation allows us to locate a phase transition between phases with an absorbing and a fluctuating stationary state. The associated universality class is that of parity conservation. We also report on a more recent study of asynchronous updates applied to the yeast cell–cycle network. Compared to the synchronous update, the basin of attraction of the largest attractor considerably shrinks and the convergence to the biological pathway slows down and is less dominant. Both examples illustrate how sensitively the stationary states and the properties of attractors can depend on the updating mode of the algorithm.

PACS numbers: 05.70.Ln, 05.50.+q, 64.90.+b

(Some figures in this article are in colour only in the electronic version)

1. Introduction

In the context of statistical physics of phase transitions the dependence of stationary states on the updating algorithm was discussed in various systems. In the NEKIM(CA) (the nonequilibrium kinetic Ising model and its cellular automaton version [1]) Glauber

and Kawasaki dynamics were combined to study temperature-driven nonequilibrium phase transitions. Here the stationary states depend on the combination of both types of dynamical processes. Also the phase diagrams of the Hopfield neural network [2] and the Blume–Emery–Griffiths model [3] depend on the updating mode, while those of the Q-state Ising model [3, 4] and the Sherrington–Kirkpatrick spin glass [5] are independent of the used scheme. Recently, there was a controversial discussion about the number of attractors that increases exponentially with the system size for synchronous update [6], and with a power for critical Boolean networks [7] for asynchronous update. This number has an important impact on the validity of S Kauffman's conjecture that the small number of dynamical attractors in Boolean networks should reflect the relatively small number of stable cell states, although many hypothetical combinations of genes exist in principle. For a systematic investigation of the dependence on the updating algorithm, we started with a smooth interpolation between the synchronous (deterministic) and the asynchronous updating modes; it was applied to the variables on the sites of a one-dimensional lattice of Ising spins (sections 2 and 3) and to the Boolean variables on the sites of the yeast cell–cycle network [8] with Boolean threshold dynamics (section 5). The results obtained for the Ising chain are published in [10] and here only reviewed in section 4. Our results on the Boolean threshold dynamics are more recent and not yet published elsewhere. They are summarized in section 6. For both systems we observe a sensitive dependence on the updating procedure. Synchronous updating of the Ising chain with ferromagnetic interaction leads to an antiferromagnetic stationary state, separated from the ferromagnetic state (obtained for the asynchronous update) by a second-order phase transition that belongs to the universality class of parity conservation (section 4). On the other hand, asynchronous updating of the threshold dynamics on the yeast cell–cycle network destroys the large basin of attraction of the G1-state of the cell cycle and the predominant convergence to the biological pathway (section 6). We compare our results to those of related models and draw the conclusions in section 7.

2. Dynamical rules for the Ising chain

We consider an Ising model on a one-dimensional lattice of length L with periodic boundary conditions and variables $\sigma_i, \sigma_i \in \{\pm 1\}$. The coupling J in the Hamiltonian $H = -J \sum_{i=1}^{L} \sigma_i \sigma_{i+1}$ between next neighbors is set to 1. Given a configuration $\Sigma(t) = \{\sigma_i(t)\}$ at time t, we select each site with probability p as a candidate to get flipped according to the rules specified below. The selected sites are $j_1, \ldots, j_m$ and m, the total number of selected sites, is a random number obeying a binomial distribution. Each of the selected sites is then updated according to the Metropolis algorithm, so that the spin of the j_vth site is flipped with probability

$$P_{j_v}(t) = \min\{1, \exp[-\beta \Delta E_{j_v}(t)]\} \tag{1}$$

for all $v \in \{1, \ldots, m\}$ and $\beta = 1/(k_B T)$, T is the temperature, k_B the Boltzmann constant and $\Delta E_{j_v}(t) = 2\sigma_{j_v}(t) \cdot [\sigma_{j_v-1}(t) + \sigma_{j_v+1}(t)]$ is the difference in local energy that a flip of σ_{j_v} would induce. In particular, for zero temperature, the only case we consider here, an increase in energy is always rejected since $P_{j_v}(t) \to 0$ for $\beta \to \infty$ and $\Delta E > 0$, while a decrease is always accepted ($P_{j_v}(t) \to 1$ for $\beta \to \infty$, $\Delta E < 0$). This implies that only spins belonging to an 'active' link (that is a link connecting spins of opposite sign) can flip and do flip if they have been selected as candidates for being updated. After one step of the algorithm the time increases as $t \to t + p = t'$ and the new configuration is $\Sigma(t') = \{\sigma_i(t); \sigma_{j_1}(t'), \ldots, \sigma_{j_m}(t')\}$, where all sites $i \neq j_1, \ldots, j_m$ have the same spin values as they have at time t, while spins
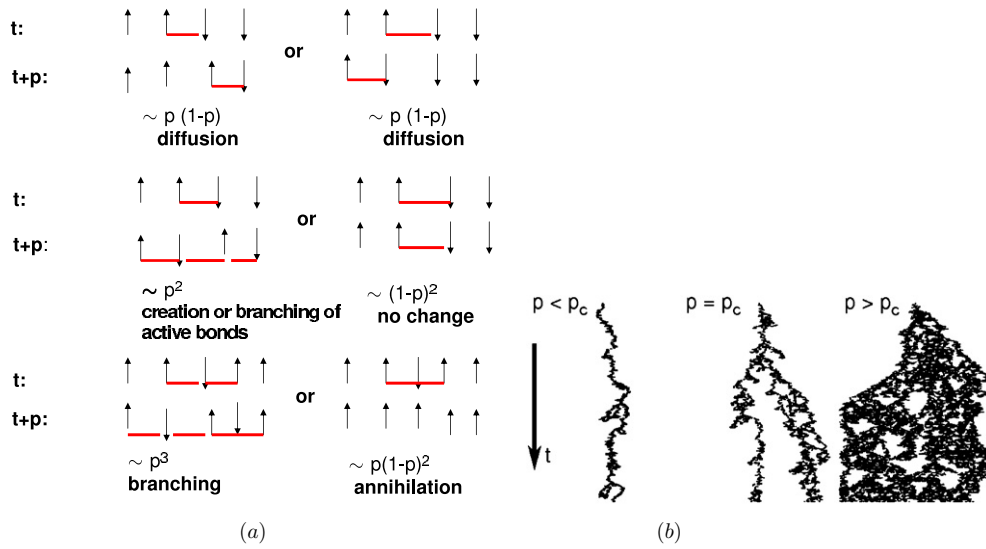
Figure 1. (*a*) Elementary processes at times *t* and *t* + *p*. (*b*) Time evolution of an initially isolated active bond (drawn in black) in the subcritical, critical, and supercritical regime. For further explanations see the text.

of the *m* selected sites which belong to active links are synchronously flipped. By varying *p*, we can now interpolate the algorithm from an asynchronous update, for *p* of the order of $1/L$, to a synchronous one for $p = 1$. For *p* of the order of $1/L$ and *L* sufficiently large (so that events of the probability $\sim 1/L^2$ are negligible) we recover the usual Metropolis algorithm. Note that for general values of *p* the total energy of the new configuration may increase with respect to the total energy of the old configuration $\Sigma(t)$. This way it happens that for $p = 1$ (synchronous update) the stationary state is an antiferromagnetic limit cycle of length two, for which the system flips between two antiferromagnetic configurations resulting from each other by an overall flip of the signs.

3. Elementary processes of the algorithm

It is instructive to classify the elementary processes which can happen during the update events since it is these processes together with their conservation law and the dimensionality of the system that determine the universality class of the phase transition as a function of *p*. As we have indicated above, only flip events which involve active links take place. They amount to diffusion (or random walk), annihilation and creation in the sense of even-branching processes, as seen in the examples of figure 1(*a*), where we have also indicated the probabilities for these events. Only active links between the spins are explicitly indicated. These processes preserve parity of active bonds, where 'parity' denotes the number of active bonds modulo 2. Since a ferromagnetic stationary state has no active bonds while such bonds are abundant in an antiferromagnetic state, it is the competition of annihilation and branching processes that determines the phase transition between the absorbing (ferromagnetic) and the active (antiferromagnetic) states. Since a synchronous updating favors branching in contrast to an asynchronous one, the transition between these stationary states can be considered as a transition between the synchronous and asynchronous updating schemes.

4. Critical point and universality class for the Ising chain

To further investigate the phase transition we first determine the critical probability p_c via the power-law decay of the order parameter at p_c, characterized by the static critical exponent δ. As an order parameter we use the density of active bonds

$$\rho = \frac{1}{2} \sum_{i=1}^{L} 1 - \sigma_i \sigma_{i+1}. \tag{2}$$

At p_c, the order parameter ρ decays like $|t|^{-\delta}$ in the large-volume limit, and for $p < p_c$ like $t^{-\alpha(p)}$ with $\alpha(p)$ a monotonically decreasing function of p with $\alpha(p) = 1/2$ for $p \to 0^+$ (as in the case of the Metropolis algorithm). For $p > p_c$ it decays with a positive curvature. A measured negative curvature for $p < p_c$ is therefore a finite-size effect. In [10] we determined p_c as the largest value leading to a non-positive curvature. The fact that p_c is larger than zero is expected and explained within a field-theoretic dynamical renormalization group by Cardy and Täuber [9].

In figure 1(b), we show the evolution of an isolated active bond of a configuration $\cdots \uparrow\uparrow\downarrow\downarrow \cdots$ in the subcritical ($p = 0.39 < p_c$), critical ($p = p_c \sim 0.41$)) and supercritical regimes ($p = 0.43 > p_c$). Active bonds are represented in black. The figure shows only the intermediate part of the chain in the vicinity of the initial link. Below and up to the critical value of p the active bonds spread over a region of finite width which stays finite also in the infinite-volume limit, since annihilation and branching are balanced, while branching dominates in the supercritical region ($p > p_c$) and leads to a spreading of active bonds all over the lattice.

In [10], we read off the dynamical exponent δ from the power-law decay of $\rho(t)$ at p_c in the large-volume limit, which is realized for $L \sim 10^4$ sites. Also in the large-volume limit we determined the dynamic exponent η from measuring the average number of active bonds $\bar{n}(t)$ as a function of time $\bar{n}(t) \sim t^\eta$.

From a finite-size scaling analysis we determined (again numerically) the dynamic exponent $z = \nu_\parallel/\nu_\perp$ by measuring the relaxation time τ needed by a finite system to reach the absorbing configuration according to $\tau \sim L^z$; $\nu_\parallel$ is the time-like correlation length, $\nu_\perp$ is the spatial correlation length.

We also measured the combination of static exponents $\beta/\nu_\perp$ from the scaling behavior of the order parameter $\rho(L, t) \sim L^{\beta/\nu_\perp} f(t/L^z)$ with f a universal function and β characterizing the order parameter near p_c according to $\rho(p) \sim |p_c - p|^\beta$. Finally, the static exponent γ follows from the finite-size-scaling behavior of the susceptibility of the order parameter at p_c. For further details of this measurement we refer to [10].

The results for the critical exponents are summarized in table 1 and compared to the exponents of the parity conservation universality class. The agreement is not surprising, since our elementary processes conserve parity as mentioned above. This universality class was identified before, in particular, for a phase transition in the NEKIM(CA) model [1]. In the NEKIM(CA) the same type of elementary processes was generated as in our algorithm, but via a combination of Glauber-spin flip dynamics and Kawasaki exchange dynamics.

5. Asynchronous update for the yeast cell–cycle network

The yeast cell–cycle network was studied in a reduced form by F Li *et al* [8]. The network contains 11 nodes plus a signal node on which the cell cycle is started by means of a cell-size signal. Nodes and links are treated as logic-like operations. Variables assigned to nodes take

Table 1. Critical exponents of the parity conservation (PC) universality class in comparison to the exponents of the synchronous/asynchronous Ising model (SAIM) measured in [10].

	$\beta/\nu_\perp$	γ	δ	$\nu_\parallel/\nu_\perp$	η
PC	1/2	0	2/7	7/4	0
SAIM	0.51(1)	0.0	0.286(1)	1.746(2)	0.0

values +1 (active) or 0 (inactive) depending on the state of the protein. Links can be positive (chosen as +1 in [8]) or negative (chosen as −1) depending on their positive or negative regulation between the proteins, respectively. Time evolves in discrete steps. States at time step $t+1$ are determined by the protein states at former time t in a deterministic way according to the following rules of threshold dynamics:

$$s_j(t+1) = \begin{cases} 1 & > 0 \\ 0 & \text{if} \quad \sum_j a_{jl}s_l(t) < 0 \\ s_j(t) & = 0, \end{cases} \tag{3}$$

where a_{jl} is either chosen as +1 or −1, depending on the assigned value to the link. For nodes which are not negatively regulated by other nodes, self-degradation is introduced. Li *et al* analyzed the phase space with the exciting result that 86% of all 2^{11} initial states converge to one and the same fixed-point configuration for which the protein states correspond to the cell phase G1. Moreover, the convergence of the states which are attracted by the G1-state follows dominantly a biological pathway whose intermediate states can be identified with the excited G1, S, G2, M and back to the stationary G1 phase of the cell cycle. (So the cell cycle is initiated by exciting the fixed point G1 by an external signal, this excited state then goes back to the stationary G1 via the intermediate states of the cell cycle; without excitation the system remains in the stationary G1 until the next signal for cell division arrives.) The convergence along paths transverse to the biological path is rather fast. As Li *et al* showed, their results are very stable against deletion of interaction arrows, flips of signs, change of certain dynamical rules, weights a_{ij}, protein lifetimes and replacement of the cell–cycle checkpoints. Anyway, it is striking that a dynamics as simple as the Boolean threshold dynamics is able to reproduce stable states which can be identified with the phases of the cell cycle.

We were therefore interested in how these results depend on the synchronous updating for which all 11 proteins are updated at the same time. As in the case of the Ising chain, we decide for each node with probability p whether the node is updated or not. Time proceeds in units of p, so that $t' = t + p$ with $p = 1/2, 1/3\ldots$ in order to obtain integer values for the labels of time steps. If N denotes the total number of nodes and p is chosen as $1/N$, the updating corresponds to the fully asynchronous case of $p = 1/L$ in the Ising chain, here $N = 11$. Once a node is selected as a candidate, it is updated according to the rules 3.

6. Phase space and biological pathway

As in [8], we call START the configuration corresponding to an 'excited' G1 state, in Boolean variables given by $(1, 0, 0, 0, 1, 0, 0, 0, 1, 0, 0)$. It differs from the stationary G1 state in the first component from the left, which is 0 for the stationary state. For the deterministic update ($p = 1$), starting from the excited state, one ends up in the stationary G1 state. It is interesting to count the number of trajectories starting from START which still fall into the G1 state when we vary the degree of asynchronous update as parameterized by p. The fraction of these trajectories over all trajectories is called $B(p)$ and plotted in figure 2. $B(p)$ first decreases with p and later increases a little for small values of p. The slight increase is due to direct
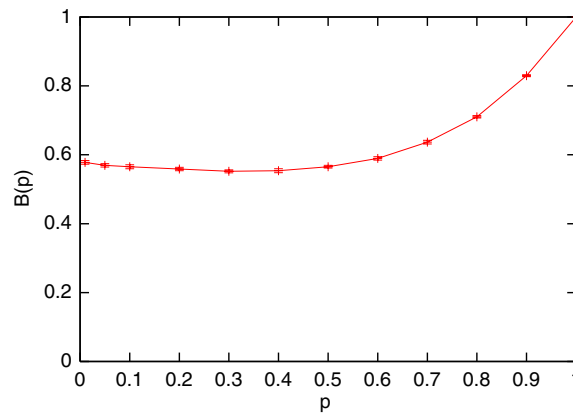
Figure 2. The fraction of the trajectories, starting from the START configuration, that fall into the stationary G1 phase as a function of the interpolation parameter p with $p = 1$ for fully synchronous update and $p = 1/11$ for fully asynchronous update. Note that we do not need to choose p as rational numbers here, since we do not follow the intermediate time steps, but examine just the final states of the trajectories.

Table 2. Size of the basins of attraction for fixed points of the cell–cycle network for synchronous ($p = 1$) and asynchronous ($p = \frac{1}{11}$) updates.

Syn	Async	Cln3	MBF	SBF	Cln1,2	Cdh1	Swi5	Cdc20	Clb5,6	Sic1	Clb1,2	Mcm1
86.1%	56.4%	0	0	0	0	1	0	0	0	1	0	0
7.4%	12.5%	0	0	1	1	0	0	0	0	0	0	0
5.3%	7.6%	0	1	0	0	1	0	0	0	1	0	0
0.4%	18.1%	0	0	0	0	0	0	0	0	1	0	0
0.3%	2.3%	0	1	0	0	0	0	0	0	1	0	0
0.3%	1.8%	0	0	0	0	0	0	0	0	0	0	0
0.05%	1.3%	0	0	0	0	1	0	0	0	0	0	0

transitions from START to the stationary G1 state, which is forbidden for the synchronous update, but possible for the asynchronous one, and more frequently occurring for small values of p.

Table 2 lists the seven Boolean configurations corresponding to seven attractor states and the absolute size of their basin of attraction for synchronous ($p = 1$) and asynchronous ($p = 1/11$) updates.

Moreover, the nice feature of the fast convergence of all states out of the basin of attraction to G1 toward the biological pathway (observed for the synchronous update) is lost for the asynchronous update. Starting again from all configurations out of the basin of attraction for the G1 state, the convergence slows down and more transitions exist to G1 which do not allow a sensible biological interpretation. A quantitative analysis of this feature will be presented elsewhere.

7. Conclusions

We have seen two examples of dynamical systems on networks (the regular chain with Ising spins and the yeast cell–cycle network with threshold dynamics) for which the stationary states and the stability properties of attractors sensitively depend on the updating mode. In both

systems we tuned the updating scheme from a fully deterministic (synchronized) one to an asynchronous mode via the probability p of selecting candidates for an update. The systematic interpolation between the synchronous and asynchronous updating revealed a phase transition for the Ising system that led to a qualitative change in the stationary states. Beyond this transition ($p > p_c$) the stationary state shows no remnants of the original (ferromagnetic) interaction entering the dynamical rules. In general, none of the extreme cases ($p = 1$ or $p = 1/L$) can be attested to be physically more relevant than the other. While a fully synchronous update may appear unrealistic in view of the omnipresent noise in biological systems, the (nearly) synchronous update seems to be biologically relevant in the yeast cell–cycle network, since the basin of attraction is quite large and the convergence to the biological pathway is quite fast, both being desired features in this context. The order in a designed cyclic process matters. In a more noisy situation, an asynchronous algorithm may be more realistic. Therefore, in general, the updating mode should be adapted to the concrete biologically relevant dynamics. From the physics' point of view, it would be interesting to identify the common features of dynamical processes which are responsible for their (in)sensitivity to the order of updating events.

Acknowledgments

References

[1] Menyhárd N and Ódor G 1995 *J. Phys. A: Math. Gen.* **28** 4505
     Ódor G and Menyhárd N 2006 *Phys. Rev.* E **73** 036130
[2] Hopfield J J 1982 *Proc. Natl Acad. Sci. USA* **79** 2554
     Fontanari J F and Köberle R 1988 *J. Phys.* **49** 13
[3] Bollé D and Busquets Blanco J 2005 *Eur. Phys. J.* B **47** 281
[4] Potts R B 1952 *Proc. Camb. Phil. Soc.* **48** 106
[5] Nishimori H 1997 *TITECH Report*
[6] Samuelsson B and Troein C 2003 *Phys. Rev. Lett.* **90** 098701
[7] Drossel B, Mihaljev T and Greil F 2005 *Phys. Rev. Lett.* **94** 088701
[8] Li F, Long T, Y Lu, Ouyang Q and Tang C 2004 *Proc. Natl Acad. Sci. USA* **101** 4781
[9] Cardy J and Täuber U C 1996 *Phys. Rev. Lett.* **77** 4780
[10] Radicchi F, Vilone D and Meyer-Ortmanns H 2007 *J. Stat. Phys.* **129** 593